

# Rothamsted Repository Download

## A - Papers appearing in refereed journals

Menezes-Blackburn, D., Sun, J., Lehto, N. J., Zhang, H., Strutter, M., Giles, C. D., Darch, T., George, T. S., Shand, C., Lumsdon, D., Blackwell, M. S. A., Wearing, C., Cooper, P., Wendler, R., Brown, L., Al-Kasbi, M. and Haygarth, P. M. 2019. Simultaneous Quantification of Soil Phosphorus Labile Pool and Desorption Kinetics Using DGTs and 3D-DIFS. *Environmental Science & Technology*. 53 (12), pp. 6718-6728.

The publisher's version can be accessed at:

- <https://dx.doi.org/10.1021/acs.est.9b00320>

The output can be accessed at: <https://repository.rothamsted.ac.uk/item/8wx44>.

© 14 May 2019, Please contact [library@rothamsted.ac.uk](mailto:library@rothamsted.ac.uk) for copyright queries.

# Simultaneous Quantification of Soil Phosphorus Labile Pool and Desorption Kinetics Using DGTs and 3D-DIFS

Daniel Menezes-Blackburn,<sup>\*,†,‡,§</sup> Jiahui Sun,<sup>‡</sup> Niklas J. Lehto,<sup>§</sup> Hao Zhang,<sup>‡,§</sup> Marc Stutter,<sup>‡,||</sup> Courtney D. Giles,<sup>||</sup> Tegan Darch,<sup>⊥</sup> Timothy S. George,<sup>||</sup> Charles Shand,<sup>||</sup> David Lumsdon,<sup>||</sup> Martin Blackwell,<sup>⊥</sup> Catherine Wearing,<sup>‡</sup> Patricia Cooper,<sup>||</sup> Renate Wendler,<sup>||</sup> Lawrie Brown,<sup>||</sup> Mohammed Al-Kasbi,<sup>#</sup> and Philip M. Haygarth<sup>‡</sup>

<sup>†</sup>Department of Soils, Water and Agricultural Engineering, CAMS, Sultan Qaboos University, PO Box 34, Al-khod 123, Sultanate of Oman

<sup>‡</sup>Lancaster University: Lancaster Environment Centre, Lancaster, LA1 4YQ, U.K.

<sup>§</sup>Department of Soil and Physical Sciences, Lincoln University, Christchurch, New Zealand

<sup>||</sup>The James Hutton Institute, Aberdeen, AB15 8QH and Dundee, DD2 5DA, Scotland, U.K.

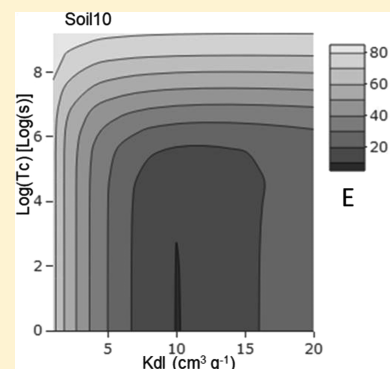
<sup>⊥</sup>Rothamsted Research: North Wyke, Okehampton, Devon EX20 2SB, U.K.

<sup>#</sup>Ministry of Environment and Climate Affairs, P.O. Box: 323, Muscat 100, Sultanate of Oman

## Supporting Information

**ABSTRACT:** The buffering of phosphorus concentrations in soil solution by the soil-solid phase is an important process for providing plant root access to nutrients. Accordingly, the size of labile solid phase-bound phosphorus pool and the rate at which it can resupply phosphorus into the dissolved phase can be important variables in determining when the plant availability of the nutrient may be limited. The phosphorus labile pool ( $P_{\text{labile}}$ ) and its desorption kinetics were simultaneously evaluated in 10 agricultural UK soils using the diffusive gradients in thin-films (DGT) technique. The DGT-induced fluxes in the soil and sediments model (DIFS) was fitted to the time series of DGT deployments (1–240 h), which allowed the estimation of  $P_{\text{labile}}$  and the system response time ( $T_c$ ). The  $P_{\text{labile}}$  concentration was then compared to that obtained by several soil P extracts including Olsen P, FeO-P, and water extractable P, in order to assess if the data from these analytical procedures can be used to represent the labile P across different soils. The Olsen P concentration, commonly used as a representation of the soil labile P pool, overestimated the desorbable P concentration

by 6-fold. The use of this approach for the quantification of soil P desorption kinetic parameters found a wide range of equally valid solutions for  $T_c$ . Additionally, the performance of different DIFS model versions working in different dimensions (1D, 2D, and 3D) was compared. Although all models could provide a good fit to the experimental DGT time series data, the fitted parameters showed a poor agreement between different model versions. The limitations of the DIFS model family are associated with the assumptions taken in the modeling approach and the three-dimensional (3D) version is here considered to be the most precise among them.



## INTRODUCTION

Among all plant macronutrients, phosphorus (P) is conceivably the one whose availability for plant uptake from soils is most limited, due to its strong interaction with the soil solid phase.<sup>1</sup> In order to maintain soil solution P at sufficient levels for plant growth, P fertilizers are usually applied to agricultural soils in doses much greater than that equivalent to plant net uptake.<sup>2</sup> In many soils, this excessive use of P fertilizers has led to an accumulation of a large (and mostly plant unavailable) pool of total soil P. Overfertilized soils present a large environmental risk especially that associated with nutrient-rich particulate matter in runoff leading to the eutrophication of receiving waters.<sup>3</sup> Overapplication of P fertilizer is largely the result of poor fertilizer application rate recommendations,

which are based on often unreliable or inappropriate measurements of plant available P. Therefore, developing reliable and accurate methods of assessing plant available P in soils is the first step toward improving the efficiency of fertilizer recommendations in support of agricultural sustainability.

Plant roots quickly deplete the dissolved P in the rhizosphere, which can induce a diffusive flux of P toward the roots and resupply from a pool of P sorbed to local soil solid phases. The amount of “plant bioavailable P” in a soil is

**Received:** February 2, 2019

**Revised:** May 12, 2019

**Accepted:** May 14, 2019

**Published:** May 14, 2019

therefore a function of the soil's capacity to supply P from the porewater, and the P that can desorb or be solubilized in response to the depletion, within a time scale that provides a nutritional benefit to the plant. Commonly used approaches to assess plant bioavailable P in soils involve an equilibrium-based method that quantifies P in different soil extracts, such as Olsen P (0.5 M NaHCO<sub>3</sub>) and Bray1-P (0.025 M HCl; 0.03 M NH<sub>4</sub>F).<sup>4,5</sup> However, the ability of these methods to sample the pool of plant bioavailable P is extremely variable<sup>6,7</sup> and, consequently, there is little consensus on how this pool can be accurately measured across different soils. Diffusive gradient in thin films (DGT) uses a dynamic approach to sample a fraction of soil P, which emulates to some extent the continuous root depletion of soil solution P, and this method has been proposed as a better estimate of plant available P in comparison to other soil P tests.<sup>8,9</sup> The similarities of DGTs to plant root behavior and its usefulness to study soil P bioavailability was reviewed by Degryse et al. (2009).<sup>10</sup>

The combination of DGTs, diffusive equilibrium in thin films (DET) and DGT-induced fluxes in soil and sediments model (DIFS) was proposed by Menezes-Blackburn et al.<sup>11</sup> to assess intrinsic P mobility properties of different agricultural soils. In this process the Olsen P extractable concentration was used as an estimation of the "desorbable" P concentration. However, this approach was subject to two key uncertainties that arose from (1) the intrinsic differences in how, and the extent to which, the Olsen P extraction and DGT sample the soil solid phase bound P, and (2) the error in modeling diffusive transport to a DGT in only one dimension.

There are currently three versions of the DIFS model. The first version describes the diffusive transport of solute from a soil into a DGT device and the sorption/desorption reactions in the soil in only a single spatial dimension (1D DIFS),<sup>12</sup> while subsequent versions have exploited improved computer processing power and expanded the dimensionality to two and three dimensions (2D- and 3D-DIFS, respectively) with a view to providing improved estimations of the diffusive flux of solute from the soil to the DGT probe.<sup>13</sup> The combination of more powerful modeling approaches with time series of DGT deployments in soils will enable the estimation of the equilibrium partitioning coefficient  $K_{dl}$  that describes the relative concentrations of P in the solution phase and P sorbed to the solid phase that can respond to localized depletion in the porewater within the time scale of the measurement, as well as the desorption rate constant for P from the labile solid phase ( $k_{-1}$ ).<sup>14,15</sup> Herein, the sum concentrations of the two components of  $K_{dl}$  is defined as the labile P pool in a soil ( $P_{labile}$ ).

In this work the 3D-DIFS model developed by Sochaczewski et al. (2007)<sup>13</sup> was extended further to provide the most accurate model representation of the commonly used DGT probe geometry and its contact with soil to date. The adapted 3D-DIFS model and publicly available 1D- and 2D-DIFS models were used together with soil deployments of DGT and DET devices to estimate the rate constants of P interchange between soil solid phase and soil solution. The aim of this study was to determine key parameters governing the resupply of P across a range of agricultural soils. To achieve this aim we sought to (a) simultaneously estimate the soil phosphorus  $K_{dl}$  and  $k_{-1}$  by fitting the DIFS model to a DGT time series; (b) use the fitted  $K_{dl}$  to estimate the soil labile P (desorbable concentration) and compare it to internationally recognized, standard agronomic soil P extraction tests; and (c) evaluate the

accuracy with which different versions of the DIFS model can be used to interrogate these parameters.

## MATERIALS AND METHODS

**Selection of Soil Samples.** Samples were from 10 UK agricultural soils and were previously characterized for pH, oxalate extractable Al and Fe, soil organic carbon, microbial biomass P, total P and inorganic P in NaHCO<sub>3</sub> (Olsen), NaOH, citric acid, and water extractable P concentrations (Supporting Information (SI) Table S1 and in Stutter et al., 2015).<sup>20,11</sup> These 10 soils are a subset of the 32 soils considered by Menezes-Blackburn et al. (2016).<sup>11</sup> They were chosen to provide a broad spectrum of UK agricultural soils, by targeting those with a range of Olsen P values from 15 to 185 mg L<sup>-1</sup>, while avoiding those with extreme textures or organic matter concentrations.

**Gel Preparation and Assembly of DGT and DET Devices.** The DGT and DET probes were assembled in the commonly used DGT "piston probe" housings, designed for soil deployment (DGT Research Ltd., Lancaster-UK). Diffusive gels (0.78 mm thick) were placed on top of a ferrihydrite containing gel layer, and overlain with a 0.13 mm thick poly(ether sulfone) filter (0.45 μm) for physical protection. The filter layer has been shown to behave as an extension of the diffusive layer.<sup>21</sup> The DET devices contained only the diffusive gel (0.78 mm thick) and the membrane filter tightly packed into a plastic support with similar dimensions to the ones used for the DGTs. The diffusive gels containing acrylamide cross-linker (DGT Research Ltd., Lancaster-UK) were prepared and cast according to Zhang and Davison (1995).<sup>21</sup> The phosphate-binding layer was prepared using the approach developed by Santner et al. (2010).<sup>22</sup> Briefly, diffusive gels (0.78 mm thick) were incubated for 2 h in 0.1 mM FeCl<sub>3</sub> and then placed in a freshly prepared 0.05 M 2-(*N*-morpholino) ethanesulfonic acid (MES) buffer, adjusted to pH 6.7, for 30 min to precipitate ferrihydrite within the gel. The gels were then hydrated over 24 h with ultrapure water (ASTM Type I, resistivity 18.2 MΩ) during which the water was changed several times. After hydration, the gels were stored at 4 °C in 0.01 M NaNO<sub>3</sub> until the probes were assembled.

**DGT and DET Deployment.** Five replicates (100 g) of each air-dried soil sample were adjusted to approximately 50% water holding capacity (WHC) with ultrapure water, 3 days before DGT and DET deployment. Twenty four hours before deployment, the soil slurry was prepared by mixing and continuously adding ultrapure water until maximum retention (MR) was reached. A visual assessment of soil malleability and the glistening of water on the soil surface was used to determine MR. This subjective criterion of setting maximum water retention in the slurry was verified by Menezes-Blackburn et al. (2016).<sup>11</sup> At MR, the soil pores were assumed to be filled with water and that no air was trapped in the soil slurry. The final moisture concentration was used to determine the particle concentration,  $P_c$  (ratio between dry weight and soil solution) and porosity (% of volume occupied by water), and were then used to calculate the soil tortuosity using the equation proposed by Boudreau (1996) and Harper et al. (1998).<sup>23,24</sup> Immediately after slurry preparation, DET probes were deployed in each one of the five replicates of each soil by gently pressing the devices against the soil slurry, ensuring complete surface contact. After 24 h the DET devices were retrieved. The DGT probes were deployed in the same fashion.

The DGT probes were deployed across a range of times (1, 2, 4, 6, 24, 48, 72, 144, 192, and 240 h) to provide a temporal dynamic of P mass supply from the soils to the DGT probes. The ambient temperature was continuously monitored during the deployments to allow for accurate estimates of diffusion coefficients. The shorter deployment times were used to increase the level of detail in the first 48 h of the *R* time series. At the end of each deployment, the ambient temperature was recorded and replicate DGT devices were removed and rinsed with ultrapure water to remove any adhering soil particles, before the probes were disassembled. The ferrihydrite gels from the DGTs and the diffusive gels from the DETs were retrieved and eluted overnight with 2 mL 0.25 M H<sub>2</sub>SO<sub>4</sub> before analysis. Three nondeployed DGT and DET “blanks” were prepared concurrently with each deployment and treated identically to the devices deployed on the soil samples. The concentration of the molybdate-reactive P (inorganic P) in subsamples of the DGT and DET eluents were measured colorimetrically as described by Murphy and Riley (1962)<sup>25</sup> using 96 well microplates. The analysis was carried out using a Multiskan spectrophotometer (Thermo Fisher Scientific Inc., UK).

**Calculation of DGT-Derived Parameters.** The DGT binding layer introduces a sink for P in the soil solution, which induces a well-defined diffusive flux from the soil through the diffusive gel and into the binding layer. The magnitude of this flux is determined throughout the deployment by the interfacial concentration, which is in turn determined by the balance between (i) the demand for solute by the DGT probe and (ii) the soil’s ability to resupply solute to the device interface. The time-averaged concentration of dissolved P at the DGT device interface for each deployment time,  $P_{DGT,i}$  was calculated using eq 1.<sup>21</sup>

$$P_{DGT,i} = \frac{M_i \times \delta_{MDL}}{D_{g,i} \times A_E \times t_i} \quad (1)$$

where  $M_i$  is the mass of P accumulated by the DGT binding layer after deployment time  $i$  ( $t_i$ ),  $A_E$  is the effective surface area of the DGT sampling window (3.08 cm<sup>2</sup>),  $\delta_{MDL}$  is the total thickness of the material diffusive layer (MDL, includes the diffusive gel layer and the filter membrane), and  $D_{g,i}$  is the temperature-adjusted average diffusion coefficient of P in the diffusive gel over the deployment. The index *R* was calculated for each deployment time, as the DGT-determined P concentration at the device interface, relative to the DET determined bulk solution P concentration DET at the start of the deployment (eq 2).

$$R = \frac{P_{DGT,i}}{P_{DET}} \quad (2)$$

The *R*-index provides an objective criterion that describes the capacity of the soil to supply P to the DGT probe over the considered deployment time. This capacity is determined by a combination of diffusive flux, and the rates at which different processes can resupply P to the solution phase when it has been depleted by the DGT.

**Numerical Modeling of DGT Deployments Using DIFS.** The 2D-DIFS model proposed by Sochaczewski et al. (2007)<sup>13</sup> was adapted to provide an improved representation of solute fluxes from soils into the DGT device. Following the approach developed by Santner et al. (2015),<sup>26</sup> a 2D-axisymmetric model was created using the COMSOL Multi-

physics (v. 5.1; Comsol Inc., Stockholm, Sweden) finite element modeling framework. The model domain was defined as a partial cross-section along the axis perpendicular to the ferrihydrite gel-diffusive gel interface, with its origin at the center of the interface. The domain included the MDL and a “cylinder” of soil that could potentially be sampled by the DGT (SI Figure S1). The model solved the partial-differential equations describing diffusion within the 2D-axisymmetric geometry and thus simulated diffusive fluxes within the soil and the MDL of the DGT probe in 3D. The model simultaneously considered the interaction of P between solid and solution phases in the soil.

As previously discussed, the model does not consider the binding (ferrihydrite) layer as a model subdomain as such. Instead, the binding of dissolved P by the ferrihydrite is simulated by imposing a zero-concentration boundary condition. The flux of P into the ferrihydrite gel of the DGT probe is integrated over the simulated deployment time and length of the ferrihydrite boundary layer considered, but expanded to 3D by calculating a revolution surface about the center of the ferrihydrite gel interface.<sup>26</sup> The boundary conditions of the model are shown in the Supporting Information.

The principles governing solute dynamics between soil solid and solution phases were identical to those employed previously and described briefly here.<sup>11,14,15</sup> The model considers the interaction between dissolved P ( $P_{sol}$ ) and sorbed P that is considered to be labile within the time of the DGT deployment ( $P_{sorbed}$ ) to follow first order exchange kinetics (eq 3),



where the rates at which the two species’ concentrations change are defined by the rate constants of adsorption ( $k_1$ ) and desorption ( $k_{-1}$ ), the concentrations of P in the sorbed and species and the particle concentration ( $P_C$ ) (eq 4 and 5).

$$\frac{\partial [P_{sol}]}{\partial t} = -k_1 \times [P_{sol}] + (k_{-1} \times P_C \times [P_{sorbed}]) \quad (4)$$

$$\frac{\partial [P_{sorbed}]}{\partial t} = \frac{k_1 \times [P_{sol}]}{P_C} - (k_{-1} \times [P_{sorbed}]) \quad (5)$$

The rate constants can be used along with the particle concentration in the soil ( $P_C$ ) to define the linear sorption isotherm ( $K_{dl}$ ) that describes the partitioning of P between the sorbed and dissolved phases, (eq 6).

$$K_{dl} = \frac{[P_{sorbed}]}{[P_{sol}]} = \frac{1}{P_C} \times \frac{k_1}{k_{-1}} \quad (6)$$

The rate at which the sorbed and dissolved P can equilibrate is expressed by eq 7,

$$T_C = \frac{1}{k_1 + k_{-1}} \quad (7)$$

where  $T_C$  (s) is the time needed for  $P_{sorbed}$  and  $P_{sol}$  to reach approximately 63.2% of their equilibrium values (asymptotic approach to equilibrium, 63.2%  $\approx 1-1/e$ ), if  $P_{sol}$  was depleted to zero.<sup>27</sup>

By constraining the variables that describe diffusion in the soil matrix using well-established formulas that describe diffusion in porous media, and the physical geometry of the

**Table 1. 3D DIFS Derived Parameters: Diffusive only  $R$  ( $R_{\text{diff}}$ ); Relative Resupply from Solid Phase at 24 h ( $R-R_{\text{diff}}$ ); Soil P Effective Concentration ( $P_E$ ); Fitted  $K_{\text{dl}}$  with Its Range of Minimum Error Solutions; Fitted  $T_c$  with Its Range of Minimum Error Solutions; Desorbable P ( $P_{\text{labile}}$ ) Calculated from the Fitted  $K_{\text{dl}}$ ; Rate Constants of Sorption ( $k_1$ ) and Desorption ( $k_{-1}$ ) Calculated from the Fitted  $T_c$**

soil	$R_{\text{diff}}$	$R-R_{\text{diff}}$ (at 24 h)	$P_E$			$K_{\text{dl}}$		$T_c$		$P_{\text{labile}}$ (mg kg <sup>-1</sup> )	$k_1$ (s <sup>-1</sup> )	$k_{-1}$ (s <sup>-1</sup> )
			(mg kg <sup>-1</sup> )	(cm <sup>3</sup> g <sup>-1</sup> )	(range)	(s)	(range)					
1	0.12	0.19	2.41	12.55	9–13	23	1–944	11.82	$4.4 \times 10^{-02}$	$2.5 \times 10^{-03}$		
2	0.12	0.13	1.90	3.22	3–4	24	1–1202	2.97	$4.2 \times 10^{-02}$	$1.9 \times 10^{-03}$		
3	0.12	0.02	0.82	1	<1–2	18	1–1930	0.72	$5.5 \times 10^{-02}$	$1.2 \times 10^{-03}$		
4	0.11	0.03	0.75	1	<1–2	17	1–1807	0.57	$5.7 \times 10^{-02}$	$7.5 \times 10^{-04}$		
5	0.12	0.09	1.51	1	1–2	19	1–3163	0.84	$5.3 \times 10^{-02}$	$8.1 \times 10^{-04}$		
6	0.10	0.04	0.91	0.5	0.5–1	2981	1–>10 000	0.32	$3.4 \times 10^{-04}$	$1.7 \times 10^{-06}$		
7	0.10	0.10	1.92	1	<1–2	19	1–>10 000	0.93	$5.2 \times 10^{-02}$	$4.1 \times 10^{-04}$		
8	0.11	0.16	1.87	10.8	6–12	20	1–3129	8.08	$4.9 \times 10^{-02}$	$3.5 \times 10^{-04}$		
9	0.10	0.04	1.71	1	0.5–7	44 356	4000–25 000	1.18	$2.3 \times 10^{-05}$	$1.3 \times 10^{-07}$		
10	0.10	0.20	7.22	13	7–15	7	1–167	30.51	$1.4 \times 10^{-01}$	$7.1 \times 10^{-04}$		

DGT probe, it is possible to carry out a targeted analysis of how  $T_c$  and  $K_{\text{dl}}$  combine to determine  $R$  for a given DGT deployment in a certain soil using the DIFS model.<sup>15,28</sup> When experimentally determined  $R$ -values for different time periods are compared against  $R$ -values obtained from representative model simulations, where different combinations of  $K_{\text{dl}}$  and  $T_c$  are tested, it is possible to get an estimate of the two values.

Lehto et al. (2008)<sup>14</sup> proposed an error index ( $E$ ) to represent the goodness-of-fit between the modeled and experimentally determined  $R$ -values, eq 8:

$$E = 100 \times \sqrt{\sum_{i=1}^N (R_e(t_i) - R_s(t_i))^2} \quad (8)$$

where  $R_e(t_i)$  is the experimentally determined  $R$  value and  $R_s(t_i)$  is the simulated value for time  $t_i$ . This error function was calculated across a range of increasing  $T_c$  (1 to 10 000 s) and  $K_{\text{dl}}$  (1–20 cm<sup>3</sup> g<sup>-1</sup>) values. The  $E$ -values were then represented visually across the simulated ranges of  $T_c$  and  $K_{\text{dl}}$ . Since this analysis often provided a range of  $T_c$  and  $K_{\text{dl}}$  values with equally low  $E$ -values, a second order polynomial function was used to represent the relationship between  $E$ ,  $\ln T_c$  and  $K_{\text{dl}}$ . This fitted polynomial function was then minimized within range of the input  $E$  as a means to obtain a single solution to  $T_c$  and  $K_{\text{dl}}$ .

While the principles of the DIFS model have remained the same since the initial work by Harper et al. (1998), it has been well recognized that models that represent the geometry in fewer than three dimensions are likely to be subject to underestimating solute fluxes under conditions when diffusion is the dominant mode of supply from the soil. Only the 1D and 2D versions of the DIFS models are open access to the wider research community enabling their use to interpret  $P_{\text{DGT}}$  in terms of soil P desorption kinetics.<sup>11</sup> In this study, the more advanced 3D DIFS approach was used for estimating  $K_{\text{dl}}$  and  $T_c$  across the experimental soils to provide an estimate that is most likely to represent actual DGT deployments in homogenized soils. A brief comparison of the three versions of the DIFS model was performed for two soils to provide an up to date analysis of the effect of dimensionality on the estimated DGT fluxes. These soils were selected due to their different properties and highest quality of experimental data on the response of  $R$  dependence curve in time.

## ESTIMATING THE SIZE OF THE SOIL LABILE PHOSPHORUS POOL

The  $P_{\text{DGT}}$  at 24 h was converted to an effective concentration using eq 9 to represent the available P from both soil solution and the solid-phase labile pool.<sup>29</sup> This calculation is an attempt to express the  $P_{\text{DGT}}$  in the concentration ranges of the soil P pools that drive its behavior: the soil solution P and P that can desorb from the soil solid phase during the deployment (eq 9)

$$P_{E,i=24} = \frac{P_{\text{DGT},i=24}}{R_{\text{diff},i=24}} \quad (9)$$

$R_{\text{diff}}$  is the hypothetical ratio of the  $P_{\text{DGT}}$  to the concentration in soil solution if no resupply from the solid phase occurred (only pore water P diffusion).  $R_{\text{diff}}$  was calculated using the adapted 3D-DIFS dynamic numerical model of the DGT–soil system developed for this work. Input parameters of particle concentration ( $P_c$ ; ratio between the soil dry weight and soil solution, g cm<sup>-3</sup>), soil porosity ( $\phi$ ), and the diffusion coefficient of P in the soil ( $D_s$ , cm<sup>2</sup> s<sup>-1</sup>) were calculated according to Harper et al. (1998).<sup>24</sup>

The fitted  $K_{\text{dl}}$  was used for estimating the labile/desorbable P ( $P_{\text{labile}}$ , mgkg<sup>-1</sup>) concentration as in eq 10:

$$P_{\text{labile}} = P_{\text{det}} \times K_{\text{dl}} \quad (10)$$

The  $P_{\text{labile}}$  was compared to  $P_{\text{Olsen}}$  and other P concentrations determined via different extracts, as a means to assess if any of them provide a good estimate of the labile solid phase pool.

The value of  $T_c$  derived using DIFS corresponds to the time needed to bring the interfacial concentration of P,  $P_i$ , from 0 to 63% of its pseudo steady state value.<sup>24</sup> It can be used to estimate adsorption and desorption rate constants using eqs 11 and 12<sup>24,30</sup>

$$k_1 = \frac{1}{T_c} \quad (11)$$

$$k_{-1} = \frac{1}{T_c(1 + K_{\text{dl}} \times P_c)} \quad (12)$$

**Statistical Methods and Tools.** All surface plots were performed in R Studio using the ggplot2 package.<sup>31</sup> Pearson's correlation was used between independent variables and the significance of correlations was judged using standard  $t$  test (significant at  $p \leq 0.05$  and very significant at  $p \leq 0.01$ ). Where necessary, according to results of the Andersen–Darling test

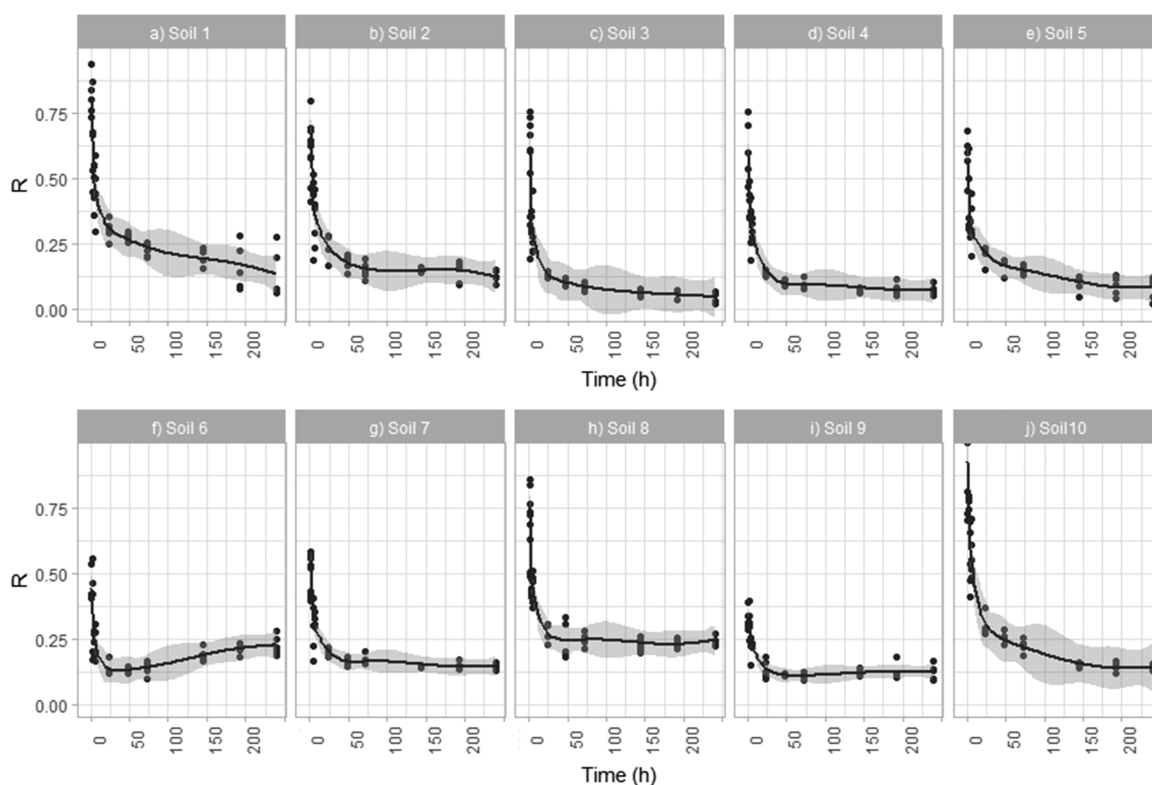


**Figure 1.** Time dependency of  $R$  curves for the experimental soils. The solid line and shaded area correspond to fitted linear regression model and its 95% confidence interval using the “natural spline” function of ggplot2 package for R Studio statistical software.<sup>31</sup>

for normality, data were  $\ln$  transformed prior to correlation analyses. Nonlinear regression functions (polynomial of degree 2) were fitted to the surface plots in order to draw patterns of general interrelation between parameters.

## RESULTS

**Experimental  $P_{\text{DET}}$ ,  $P_{\text{DGT}}$ , and  $R$  values.** The average of the measured initial  $P_{\text{DET}}$  and the  $P_{\text{DGT}}$  values across the time series (1–240 h) are displayed in Table 1. Soils 1–10 are displayed in order of increasing Olsen P concentration values. As expected, the  $P_{\text{DGT}}$  values were highest at 1 h and continuously decreased tending to stabilize in an inverse plateau at longer times (usually at 48 h), mimicking a negative power function. This trend reflects a decrease in the rate of P mass accumulation in the ferrihydrite binding layer in time. Since initial  $P_{\text{DET}}$  does not change, a similar pattern was observed to the ratio between  $P_{\text{DGT}}$  and  $P_{\text{DET}}$  ( $R$ ), which represents P concentration at the surface of the DGT device relative to the solution P concentration in the soil that has not been depleted by P diffusion to the DGT (Figure 1). In general,  $R$  values showed a steep decline from 1 to 48 h. After 48 h, this rate of decline was much lower (soils 1, 2, 3, 5, and 10) or stabilized (soils 4, 7, 8, and 9), except for soil 6 where the  $R$  values tended to increase at longer times. Possible explanations for this behavior of soil 6 could be the growth of a P mobilizing microbe or prolonged anoxic conditions. Further studies are needed to elucidate the reasons behind this unexpected behavior in soil 6. The biggest decrease in the average  $R$  values during the experiment (from 1 to 240 h) was in soil 3, from 0.63 to 0.05. It was followed by that in soil 10, with  $R$  values changed from 0.92 to 0.14. The fact that in most soils  $R$  values kept nearly constant between 48 h and 240 h

indicated that near steady-state conditions at the DGT–soil interface were reached.

**Adsorbed P and P Desorption Kinetics Obtained from 3D DIFS Model Fitted to DGT Time Series.** The distribution of error ( $E$ ) values between the 3D DIFS model output and experimental  $R$  values, for different combinations of tested  $K_{\text{dl}}$  and  $T_c$  values for the 10 soils are displayed in Figure 2. The fitted optimal  $T_c$  and  $K_{\text{dl}}$  combinations were taken as the ones where the fit between the modeled and experimental  $R$  values was the best (lowest  $E$ , Figure 2). Variation in  $T_c$  values affected the shape of the initial part of the  $R$  curve (first 48 h) while changes in  $K_{\text{dl}}$  affected the output  $R$  values at longer deployment times (72 to 240 h). The simultaneous fitting output of  $R$  values using the 3D-DIFS model proved to be a challenging process. For example, the optimum fit for soil 2 and soil 8 showed a better representation of the experimental data at the initial 24 h ( $T_c$  influenced zone), whereas in soils 4, 5, 9, and 10, the DIFS model fits the later experimental data (>72 h) better. The error surface maps between model calculated and experimental values also showed multiple combinations of  $K_{\text{dl}}$  and  $T_c$  could fit one experimental data set equally well. This was especially true for  $T_c$  values with a wide range of equally valid solutions. For example, when  $K_{\text{dl}}$  was set to  $10 \text{ cm}^3 \text{ g}^{-1}$  in soil 10, with the  $T_c$  values ranging from 1 to 25 s, the errors between DIFS-output results and experimental data ( $R$  values) were nearly constant (approximately 10).

Since the error surface maps showed a wide range of equally valid solutions for  $K_{\text{dl}}$  and  $T_c$  (Figure 2), nonlinear regression polynomial functions were fitted to the surface plots and minimized in order to find single solutions for  $K_{\text{dl}}$  and  $T_c$  for each soil (Table 1). The range of equally valid (minimum error)  $K_{\text{dl}}$  and  $T_c$  values are also displayed alongside their

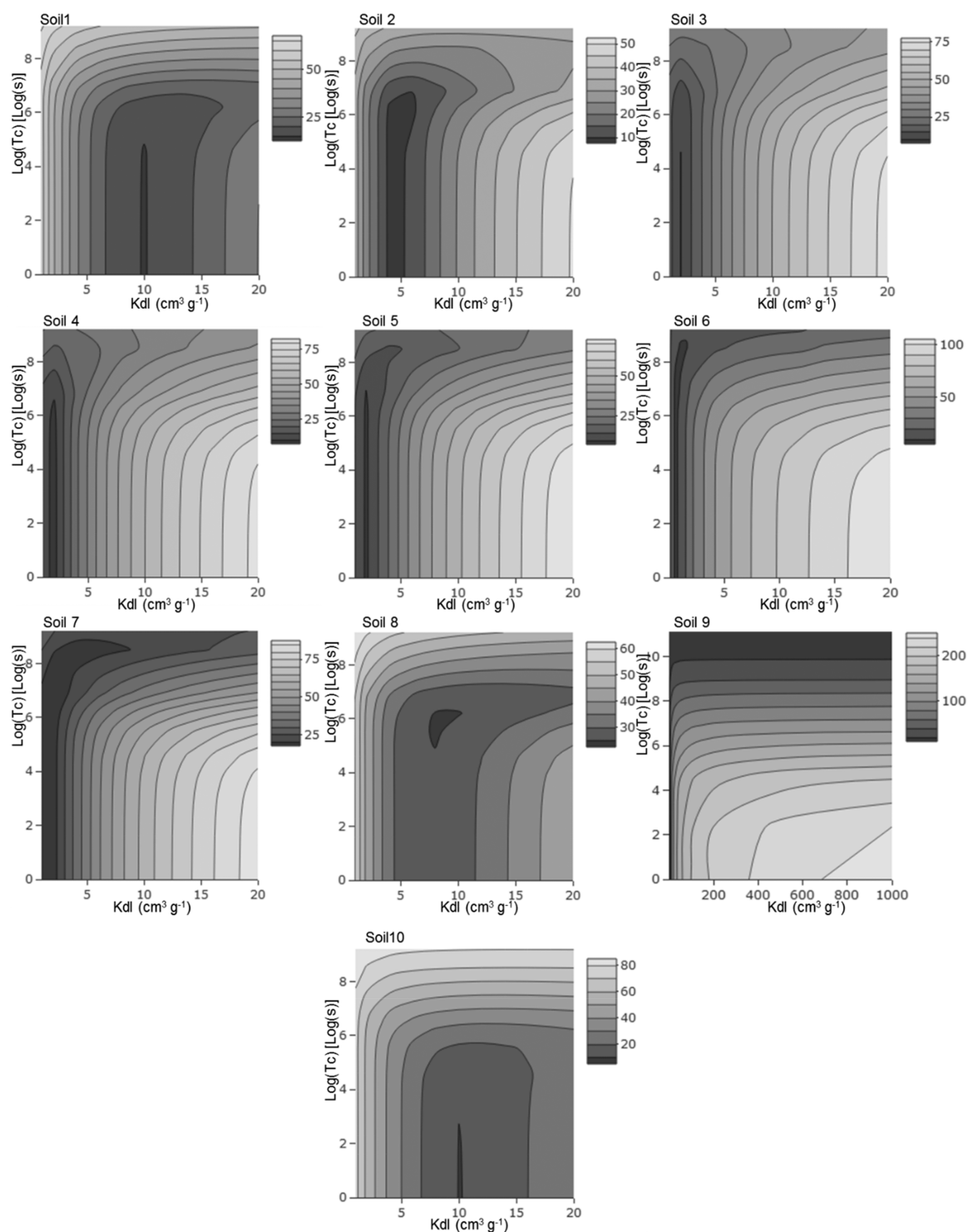


**Figure 2.** Surface contour maps of the error function between modeled and experimental  $R$  values near its minimum showing the distribution of  $K_{dl}$  and  $T_c$  values that fit the experimentally measured  $R$  data for 10 different soil samples using the 3D DIFS Model.

optimum fitted values. The  $K_{dl}$  values were used to calculate the desorbable labile P ( $P_{labile}$ ) using eq 5 and  $T_c$  values were used to calculate the rate constants of P sorption and desorption on the soil solid phase using eq 6 and 7 (Table 1). The  $R$  values at simulated diffusive only conditions ( $R_{diff}$ ) were similar for all soil samples (ranging from 0.10 to 0.12; Table 1), reflecting the small variations in porosity between different soils under the slurry conditions required for the DGT deployment. The difference between  $R$  and  $R_{diff}$  ( $R -$

$R_{diff}$ ) at 24 h was also calculated (ranging from 0.04 to 0.20; Table 1), reflecting the relative resupply of P from solid phase during the first 24 h as proposed by Menezes-Blackburn et al. (2016).<sup>11</sup>

A correlation analysis was used to examine interrelations between the  $P_{labile}$ ,  $R - R_{diff}$  and  $k_{-1}$  with soil background properties such as soil texture, pH, organic matter, and P concentration in different soil extracts (Table 2). In this analysis, only the parameters with high correlation with our

**Table 2. Pearson Correlation Coefficients between  $P_{\text{labile}}$ ,  $R-R_{\text{diff}}$ , and  $k_{-1}$  with P Concentration in Different Soil Extracts and Other Soil Background Properties (\*\* $p < 0.01$ , \* $p < 0.05$ )**

	$P_{\text{labile}}$	$R-R_{\text{diff}}$	$k_{-1}$
surface area	0.67**	0.21	-0.35
clay (%)	0.67**	0.18	-0.42*
$P_{\text{Olsen}}$	0.80**	0.44*	-0.42*
$P_{\text{FeO}}$	0.89**	0.58**	-0.14
$P_{\text{ox}}$	0.91**	0.57**	-0.17
$P_{\text{NaOH/EDTA}}$	0.88**	0.51**	-0.24
$P_{\text{tot}}$	0.93**	0.68**	0.10
$P_{\text{water}}$	0.72**	0.44*	-0.34
N (%)	-0.10	0.26	0.90**
C (%)	-0.09	0.25	0.91**

response variables were displayed. As expected, the  $P_{\text{labile}}$  was well correlated with soil P status indicators such as  $P_{\text{Olsen}}$ ,  $P_{\text{FeO}}$ , and  $P_{\text{tot}}$ , as well as with clay content and surface area. On the other hand, the desorption rate constant,  $k_{-1}$ , correlated well with soil organic matter parameters such as % soil carbon and nitrogen. Overall the coefficients of correlation between  $R-R_{\text{diff}}$  and other background soil properties were much lower than that for  $P_{\text{labile}}$  and  $k_{-1}$ , since this parameter integrates the effects of desorbable P ( $P_{\text{labile}}$ ) and the desorption kinetics ( $k_{-1}$ ).

The use of P concentration measured in different soil extracts as predictors of the desorbable P concentration ( $P_{\text{labile}}$ ) was tested using a linear regression analysis with and without setting the intercept to zero (Table 3). The linear model with

**Table 3. Linear Regression Parameters of between  $P_{\text{labile}}$  and Phosphorus Concentration in Different Soil Extracts<sup>a</sup>**

$P_{\text{ex}}$ mg kg <sup>-1</sup>	$P_{\text{ex}} = a \times P_{\text{labile}}$		$P_{\text{ex}} = a \times P_{\text{labile}} + b$		
	$a$	$r^2$	$a$	$b$	$r^2$
$P_{\text{Olsen}}$	5.82	0.29	4.18	32.6	0.63
$P_{\text{FeO}}$	4.45	0.51	3.36	21.5	0.79
$P_{\text{ox}}$	102	0.56	78.8	475	0.82
$P_{\text{NaOH/EDTA}}$	64.9	0.75	58.4	128	0.78
$P_{\text{water}}$	1.32	0.47	1.08	4.79	0.57
$P_{\text{tot}}$	125	0.23	78.0	942	0.87

<sup>a</sup> $P_{\text{ex}}$ : P concentration obtained from different soil extracts in mg kg<sup>-1</sup>.

intercept at zero ( $P_{\text{ex}} = a \times P_{\text{labile}}$ ) shows a direct relationship between the parameters, while the model without the intercept at zero ( $P_{\text{ex}} = a \times P_{\text{labile}} + b$ ) allows for the assumption that a fixed additional amount of P is extracted independently from the  $P_{\text{labile}}$  concentration. In general, all parameters showed a good capacity for the prediction of the  $P_{\text{labile}}$ . The water extractable P ( $P_{\text{water}}$ ) showed the most similar absolute values to the  $P_{\text{labile}}$  with slopes of 1.32 and 1.08 for the models with and without intercept at zero, respectively. Therefore, the water extractable P at 1:4 solid-to-liquid ratio ( $P_{\text{water}}$ ) should be used as a proxy for  $P_{\text{labile}}$  in further DGT-DIFS P analysis, instead of the previously commonly used  $P_{\text{Olsen}}$ . Soil 1 was a common outlier and the  $r^2$  from most of the Table 3 would increase significantly if this value is excluded from the analysis; for example, for the  $P_{\text{Olsen}}$  in the model without the intercept at zero the  $r^2$  would increase from 0.63 (Table 3) to 0.85 if soil 1 is excluded.

**Comparison of 1D, 2D, and 3D DIFS Models.** The data collected offered an opportunity to compare the 1D, 2D, and 3D versions of the DIFS model, although this was not a central objective. Soils 5 and 7 were selected for building the error plots between modeled and experimental data, used to visually compare model behavior and agreement (Figure 3). These two samples showed good fit between experimental and model predicted R values and had contrasting predicted  $K_{\text{d}}$  and  $T_{\text{c}}$  values, which helped to visualize the differences in error function maps and compare the model versions. The same input parameters were used throughout this analysis:  $K_{\text{d}}$  ranging from 1 to 20 cm<sup>3</sup> g<sup>-1</sup> and  $T_{\text{c}}$  ranging from 1 to 10<sup>4</sup> s. The patterns of error distribution were visually very different between the three DIFS model versions. There was reasonably good agreement between the 1D and 3D DIFS versions on the  $K_{\text{d}}$  and  $T_{\text{c}}$  solutions minimizing the error between modeled and experimental data, nevertheless the 2D version showed a greater range of  $K_{\text{d}}$  solutions and a narrower range of equally valid  $T_{\text{c}}$  values. Given the method used to calculate the E-values (eq 8), there is arguably a bias toward  $K_{\text{d}}$  and  $T_{\text{c}}$  values that provide the best overall model fit to the experimental R data in the first 48 h owing to the greater density of measurements in this period, as noted by Lehto et al. (2008).<sup>14</sup> A further sensitivity analysis targeting the latter three deployments in each soil found that the difference in  $K_{\text{d}}$  was less than 50% for soils 1, 2, 4, 5, 6, 9, and 10 (not shown). On the other hand, the measured R values in soil 3 after 48 h were lower than could be achieved by the diffusive only case in the model ( $R = 0.1$ ), suggesting that an unaccounted for process was progressively removing P from solution during the deployment in this soil. The bias resulted in an 8-fold difference in soil 7 ( $K_{\text{d}}$ : 8 cm<sup>3</sup> g<sup>-1</sup>) and a 2-fold difference in soil 8 ( $K_{\text{d}}$ : 20 cm<sup>3</sup> g<sup>-1</sup>) when focusing on the latter three deployments. These are likely to have been due to slowly desorbing solid phases contributing P into solution during the longer deployments that are not accounted for in the single-pool 3D-DIFS model. Overall, the data from the 3D DIFS model provided the best fit with experimental data (lower E-values), indicating that the 3D DIFS model used here provides the best estimates of  $T_{\text{c}}$  and  $K_{\text{d}}$  values for P in the soils considered.

## DISCUSSION

**Phosphorus Lability and Bioavailability in Soils.** The DIFS modeling approach has been previously used for the direct quantification of response time of the system ( $T_{\text{c}}$ ) directly associated with the P (de)sorption rate constants.<sup>11</sup> In order to solve the DIFS models for  $T_{\text{c}}$  alone, the distribution ratio ( $K_{\text{d}}$ ) between  $P_{\text{labile}}$  concentration associated with the soil solid phase, and its concentration in solution ( $P_{\text{DET}}$ ) is needed. The solid-to-solution distribution ratio ( $K_{\text{d}}$ ) was quantified by Menezes-Blackburn et al. (2016)<sup>11</sup> using bicarbonate extractable phosphorus ( $P_{\text{Olsen}}$ ) concentration as a proxy for the  $P_{\text{labile}}$  concentration associated with the soil matrix. The problem with this approach is that there are many methodologies available for quantifying labile desorbable/bioavailable P concentration, such as the many available agronomic P tests, each one of them returning vastly different absolute P concentration values. On the other hand, various studies have shown that DGT-derived values of P availability in soils can provide better predictions of plant yield in comparison with other commonly used P bioavailability indicators such as Mehlich-3, Bray-1, Olsen, and resin P.<sup>9,32</sup> To check the

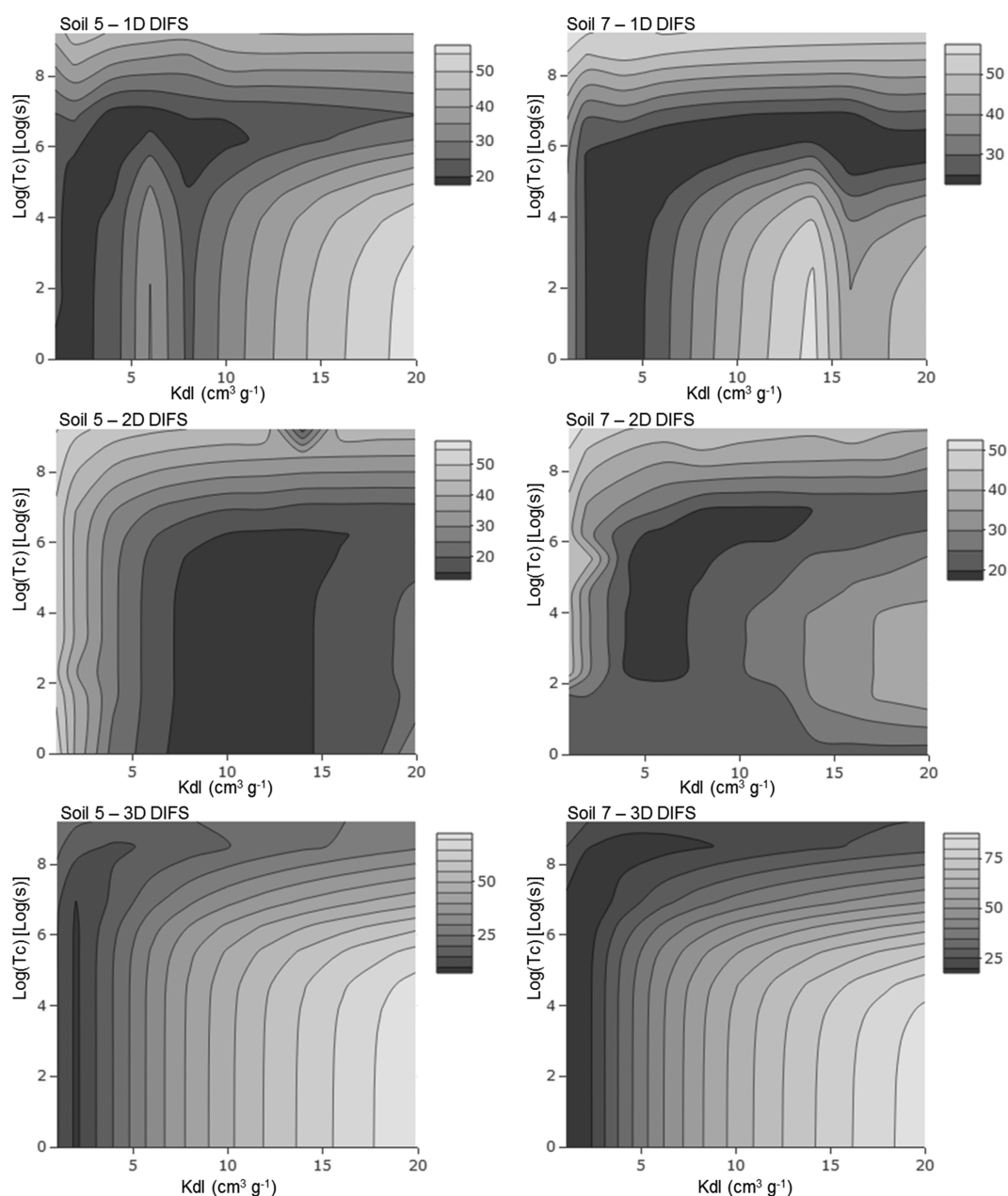


**Figure 3.** Comparison of the 1D, 2D, and 3D DIFS models error function surface maps, showing the distribution of  $K_{dl}$  and  $T_c$  values that fit the experimentally measured  $R$  data for P from soils 5 and 7.

accuracy of the approach proposed by Menezes-Blackburn et al. (2016),<sup>11</sup> time series deployments of DGTs were used to fit the DIFS model to simultaneously obtain  $T_c$  and  $K_{dl}$ .<sup>12,31</sup> Although the approach of simultaneous fit of  $T_c$  and  $K_{dl}$  is methodologically sound, it returned multiple, equally valid solutions, which is in accordance with previously described work on metals in soil.<sup>14</sup> Additionally, this analysis was biased toward the  $T_c$  increasing the uncertainties in quantifying  $K_{dl}$ , due to the greater number of experimental points on the initial 2 days of deployment, as described herein.

Our results (Table 3) indicated that the use  $P_{Olsen}$  as a proxy for  $P_{labile}$  represented a 6-fold overestimation and that the water extractable P would be a more accurate direct representation of  $P_{labile}$ . Nevertheless,  $P_{Olsen}$  and other parameters such  $P_{FeO}$  showed a good predictive capacity and can be easily transformed into  $P_{labile}$  estimations for the soils considered

by using the formulas and coefficients displayed in Table 3. This step is essential to avoid future miscalculations of desorption kinetic parameters using the methodology proposed by Menezes-Blackburn et al. (2016).<sup>11</sup> On the other hand this finding does not mean that Olsen P and other agronomic P fertility tests are not good predictors of P bioavailability to plants, since specific active root P mobilization mechanisms may increase P desorption and availability.<sup>33</sup>

As expected,  $P_{labile}$  showed a good correlation with P concentration in different soil extracts, as well as with the soil total P concentration (Table 2). These parameters represent the soil P fertility status and are most likely associated with the accumulated amount of P fertilizer inputs that these soils received through the previous years.<sup>1,2</sup> Additionally,  $P_{labile}$  showed a good correlation with soil surface area and clay

content, which are intimately interrelated. Clays, clay sized particles, and soil colloids are expected to harbor most of the P adsorption sites from which  $P_{\text{labile}}$  may be desorbed.<sup>34,35</sup>

**Phosphorus Desorption Kinetics.** The value of  $T_c$  outputs from the DIFS model simulations correspond to the time needed to bring the dissolved P concentration from near 0 to 63% of its equilibrium concentration when buffered by the labile pool of P sorbed to the solid phase.<sup>27</sup> From  $T_c$  the rate constants of sorption and desorption ( $k_1$  and  $k_{-1}$ ) were calculated using eqs 6 and 7. As previously stated, the approach taken here for minimizing the error between DIFS modeled and experimental DGT time series data was very imprecise in the estimation of  $T_c$ , as evidenced by the wide range (over 100 fold) of equally valid  $T_c$  solutions. However, the derived  $k_{-1}$  values correlated strongly with the soil N and C concentrations (Table 2). Dissolved organic matter is known to induce P desorption due to its direct competition with P for adsorption sites<sup>36</sup> thus, indicating that although imprecise, this estimation of  $T_c$  could be reflecting the behavior of the soil (de)sorption kinetics. Once a good prediction of  $P_{\text{labile}}$  is achieved using P concentration in soil extracts and formulas from Table 3, a better and simpler approach would be to use the extractable P and  $P_{\text{DET}}$  to estimate  $K_d$ , and then use it as a DIFS model input parameter for the direct estimation of  $T_c$  from 24 h DGT deployments, as proposed by Menezes-Blackburn et al. (2016).<sup>11</sup>

**Performance and Implications of Using DIFS Model to Estimate  $K_{dl}$  and  $T_c$ .** The dynamic model of the DGT–soil interaction (DGT-induced fluxes in soils and sediments; DIFS) was created in order to interpret DGT data in terms of the concomitant processes of diffusion and desorption of solute from the soil matrix.<sup>24</sup> The first version (1D DIFS) considered only linear P influx toward and perpendicular to the binding layer.<sup>24</sup> Further developments to this first version used a transect of the DGT–soil system to partly consider the contribution of lateral diffusion to the mass of analyte accumulated by the DGT device (2D DIFS), improving its accuracy and reliability.<sup>13</sup> Although the 1D and 2D DIFS models are the most widely used and the only ones publicly available, there are well-recognized limitations to these DIFS model versions: (i) they do not account for the full extent of lateral diffusion within the soil matrix in three dimensions (3D);<sup>13</sup> and (ii) they are constrained in the probe geometry that they simulate, and thus do not consider lateral diffusion within the diffusive gel layer that can affect the calculation of solute fluxes from the soil.<sup>26</sup> The 3D-DIFS model provides the most realistic simulation of P fluxes into a DGT device by accounting for diffusion within the soil and the diffusion layer in three dimensions. Nevertheless, like in the case of our study, it needs to be customized for each specific experimental condition (volume and geometry of the soil sample and DGT device) to accurately simulate the entire soil and DGT environment. In our study, the 3D DIFS version was used due to its improved accuracy on the simulation of the DGT–soil interaction, including the simulation of the complete soil volume and also considering the lateral diffusion in the diffusive layer, which is larger than the window of contact between the DGT in the soil. This becomes increasingly important with increasing depletion of dissolved P concentration away from the DGT–soil interface with time.<sup>13,37</sup> Irrespective of the model version, the combination of DGT and DIFS offer a unique opportunity to assess the basic

principles of movement kinetics of different analytes through soils and sediments.<sup>14,24,37</sup>

Our results indicated that there was a large degree of uncertainty in the process of estimating  $K_{dl}$  and  $T_c$  for P in our 10 soil samples using the 3D DIFS model. Additionally, there was poor agreement between the fitted  $K_{dl}$  and  $T_c$  between the 1D, 2D, and 3D DIFS models. Similarly to our results for P, DIFS models have been shown to occasionally have a poor fit to experimental data of metals in soil solution concentrations using DGTs<sup>28</sup> or a poor agreement between different model versions.<sup>13</sup> The limitations of the DIFS model family are usually associated with the assumptions taken in the modeling approach.<sup>38,39</sup> The first assumption, that may not always hold true, is that it considers a single pool of labile P associated with the soil solid phases. In effect, the “lability” is directly related to the soil inorganic P speciation and the affinity for these species by different colloids. Models that consider multiple pools of labile solute, with different desorption rate constants have been reported to increase the DIFS model accuracy.<sup>38</sup> Alternatively, the accuracy of these parameters could possibly be improved by fitting the model to a subset of the data.<sup>14</sup> This restriction would allow the model to fit independently the initial  $T_c$  dominated or the later  $K_{dl}$  dominated part of the time series of R curve. In our sample set, many cases were observed in which the DIFS model showed a biased better fit toward the initial  $T_c$  dominated part of the curve, due to the higher density of experimental points in the first day of deployment.

Another DIFS model assumption that may not hold true is that it uses a linear (de)sorption relationship for simplicity, because building a Langmuir type isotherm into the model would add an extra layer of complexity that would likely prevent the model from being easily used. Establishing the P concentration range under which the DIFS models can be used reliably is nevertheless important for accurate performance, especially in situations where the P saturation of the binding sites occurs either through high P concentration, or by competitive sorption of naturally occurring, low-molecular-weight, negatively charged soil organic compounds.

Despite its limitations, the use of DIFS models alongside DGT and DET to assess the kinetics of P (de)sorption and diffusion through soils has been a leap forward in the understanding of the behavior of these systems.<sup>11,31</sup> This new approach offers several advantages over other methods of solving soil P (de)sorption kinetics, among them: (i) Similar moisture content to their undisturbed conditions; (ii) use of natural P concentration range without the need for spiking; (iii) better conservation of the P chemical forms from post extraction transformations; (iv) preconcentration of soil solution P on the DGT binding layer, allowing for more accurate results.

In conclusion, the 3D DIFS model was used to interpret a time series of DGT and DET deployments in terms of soil P lability and the rate constants of P interchange between soil solid phase and soil solution. The approach was adapted from previous work related to metal desorption from sediments and soil. Our results showed that an accurate estimation of P lability (desorbable concentration) was obtained, whereas the response time of the systems and their derived rate constants of (de)sorption showed a wide range of equally valid solutions. The labile P was well correlated with soil P status indicators (such as  $P_{\text{Olsen}}$ ,  $P_{\text{FeO}}$ , and  $P_{\text{tot}}$ ), as well as with clay content and surface area, whereas the desorption rate constant was well correlated with organic matter related parameters. In general, P

concentration in different soil extracts showed a good capacity for the prediction of the labile P, and the iron oxide strip extractable P was the best performing test in this analysis. However, the water extractable P showed the most similar absolute values to the labile/desorbable P and could be used for its direct representation in future DGT studies, following the methodology proposed by Menezes-Blackburn et al. (2016).<sup>11</sup> The approach taken of using DGT time series data was very imprecise in the estimation of  $T_c$ , as evidenced by the wide range of equally valid solutions. Nevertheless, it was found to be a valid method for fact checking previous proposed methodologies while bringing valuable insights between the dynamics of P interchange between soil solid and solution phases. Refs 16 and 17.

## ■ ASSOCIATED CONTENT

### ● Supporting Information

The Supporting Information is available free of charge on the ACS Publications website at DOI: [10.1021/acs.est.9b00320](https://doi.org/10.1021/acs.est.9b00320).

Additional information as noted in the text (PDF)

## ■ AUTHOR INFORMATION

### Corresponding Author

\*E-mail: [danielblac@squ.edu.om](mailto:danielblac@squ.edu.om).

### ORCID

Daniel Menezes-Blackburn: 0000-0002-8142-9655

Hao Zhang: 0000-0003-3641-1816

### Notes

The authors declare no competing financial interest.

## ■ ACKNOWLEDGMENTS

This work was performed as part of the Organic Phosphorus Utilisation in Soils (OPUS) project, funded by Biotechnology and Biological Sciences Research Council (BBSRC) responsive mode grant (BB/K018167/1) in the UK to explore cropping strategies to target the use of recalcitrant soil Po. The James Hutton Institute receives financial support from the Rural & Environment Science & Analytical Services Division of the Scottish Government. The first author received financial support from Sultan Qaboos University through the Deanship of Research (project RF/AGR/SWAE/18/01).

## ■ ABBREVIATIONS AND SYMBOLS

$P_i$	inorganic phosphorus
DGT	diffusive gradients in thin films using ferrihydrite as a P sink at the binding layer
DET	diffusive equilibration in thin-films (DGT setup, but without the binding layer)
DIFS	“DGT Induced Fluxes in Soils and Sediments” model
$P_{DET}$ (mg l <sup>-1</sup> )	pore water (dissolved) P concentration determined using DET sampler
$P_{DGT}$ (mg l <sup>-1</sup> )	DGT estimated time averaged soil solution P concentration at the surface of DGT device
$P_E$ (mg l <sup>-1</sup> )	effective P concentration – DGT estimated soil solution P + labile $P_{labile}$ concentration

$P_{Olsen}$ (mg kg <sup>-1</sup> )	soil inorganic phosphorus concentration measured via NaHCO <sub>3</sub> extraction <sup>5</sup>
$P_{FeO}$ (mg kg <sup>-1</sup> )	soil inorganic phosphorus concentration using Fe oxide paper strip method <sup>16</sup>
$P_{ox}$ (mg kg <sup>-1</sup> )	oxalate extractable soil inorganic phosphorus <sup>17</sup>
$P_{NaOH/EDTA}$ (mg kg <sup>-1</sup> )	soil inorganic phosphorus concentration NaOH-EDTA extract at 1:20 w/v ratio <sup>18</sup>
$P_{tot}$ (mg kg <sup>-1</sup> )	soil total phosphorus concentration by NaOH fusion method <sup>19</sup>
$P_{water}$ (mg kg <sup>-1</sup> )	water extractable soil inorganic phosphorus concentration (1:4 w/v)
$P_{labile}$ (mg kg <sup>-1</sup> )	inorganic phosphorus concentration (solid phase) susceptible to desorption/solubilization by the depletion of soil solution P
$D$ (cm <sup>2</sup> s <sup>-1</sup> )	diffusion coefficient in diffusive layer of DGT device
$k_{-1}$ (s <sup>-1</sup> )	desorption rate constant
$k_1$ (s <sup>-1</sup> )	sorption rate constant
$K_{dl}$ (cm <sup>3</sup> g <sup>-1</sup> )	Equilibrium distribution coefficient between solid phase and soil solution
$R$	ratio of $P_{DGT}$ to $P_{DET}$
$R_{diff}$	ratio of $P_{DGT}$ to $P_E$ , estimated using DIFS for diffusive transport only case
$T_c$ (s)	response time of (de)sorption process

## ■ REFERENCES

- Vance, C. P.; UhdeStone, C.; Allan, D. L. Phosphorus acquisition and use: critical adaptations by plants for securing a nonrenewable resource. *New Phytol.* **2003**, *157*, 423–447.
- Syers, J.; Johnston, A.; Curtin, D. Efficiency of soil and fertilizer phosphorus use. Reconciling changing concepts of soil phosphorus behaviour with agronomic information. *FAO Fertilizer and Plant Nutrition Bulletin* 18; Food and Agriculture Organization of the United Nations: Rome, Italy, 2008.
- Menezes-Blackburn, D.; et al. Opportunities for mobilizing recalcitrant phosphorus from agricultural soils: a review. *Plant Soil* **2018**, *427*, 5–16.
- Bray, R. H.; Kurtz, L. Determination of total, organic, and available forms of phosphorus in soils. *Soil Sci.* **1945**, *59*, 39–46.
- Olsen, S. R. *Estimation of Available Phosphorus in Soils by Extraction with Sodium Bicarbonate*; United States Department Of Agriculture; Circular 939, 1954.
- Saggar, S.; et al. Development and evaluation of an improved soil test for phosphorus, 3: field comparison of Olsen, Colwell and Resin soil P tests for New Zealand pasture soils. *Nutr. Cycling Agroecosyst.* **1999**, *55*, 35–50.
- Holford, I.; Hird, C.; Lawrie, R. Effects of animal effluents on the phosphorus sorption characteristics of soils. *Soil Research* **1997**, *35*, 365–374.
- Tandy, S.; et al. The use of DGT for prediction of plant available copper, zinc and phosphorus in agricultural soils. *Plant Soil* **2011**, *346*, 167–180.
- Six, L.; Smolders, E.; Merckx, R. The performance of DGT versus conventional soil phosphorus tests in tropical soils - maize and rice responses to P application. *Plant Soil* **2013**, *366*, 49–66.
- Degryse, F.; Smolders, E.; Zhang, H.; Davison, W. Predicting availability of mineral elements to plants with the DGT technique: a review of experimental data and interpretation by modelling. *Environ. Chem.* **2009**, *6*, 198–218.
- Menezes-Blackburn, D.; et al. A holistic approach to understanding the desorption of phosphorus in soils. *Environ. Sci. Technol.* **2016**, *50*, 3371–3381.

- (12) Harper, M. P.; Davison, W.; Tych, W. DIFS - a modelling and simulation tool for DGT induced trace metal remobilisation in sediments and soils. *Environ. Modell. Softw.* **2000**, *15*, 55–66.
- (13) Sochaczewski, A. U.; Tych, W. o.; Davison, B.; Zhang, H. 2D DGT induced fluxes in sediments and soils (2D DIFS). *Environ. Modell. Softw.* **2007**, *22*, 14–23.
- (14) Lehto, N.; Sochaczewski, A.; Davison, W.; Tych, W.; Zhang, H. Quantitative assessment of soil parameter (KD and TC) estimation using DGT measurements and the 2D DIFS model. *Chemosphere* **2008**, *71*, 795–801.
- (15) Ernstberger, H.; Zhang, H.; Tye, A.; Young, S.; Davison, W. Desorption kinetics of Cd, Zn, and Ni measured in soils by DGT. *Environ. Sci. Technol.* **2005**, *39*, 1591–1597.
- (16) Chardon, W.; Menon, R.; Chien, S. Iron oxide impregnated filter paper (P i test): A review of its development and methodological research. *Nutr. Cycling Agroecosyst.* **1996**, *46*, 41–51.
- (17) Farmer, V.; Russell, J.; Smith, B. Extraction of inorganic forms of translocated Al, Fe and Si from a podzol Bs horizon. *J. Soil Sci.* **1983**, *34*, 571–576.
- (18) Turner, B. L.; Mahieu, N.; Condon, L. M. The phosphorus composition of temperate pasture soils determined by NaOH-EDTA extraction and solution <sup>31</sup>P NMR spectroscopy. *Org. Geochem.* **2003**, *34*, 1199–1210.
- (19) Smith, B.; Bain, D. A sodium hydroxide fusion method for the determination of total phosphate in soils. *Commun. Soil Sci. Plant Anal.* **1982**, *13*, 185–190.
- (20) Stutter, M. I.; et al. Land use and soil factors affecting accumulation of phosphorus species in temperate soils. *Geoderma* **2015**, *257*, 29–39.
- (21) Zhang, H.; Davison, W. Performance characteristics of diffusion gradients in thin films for the in situ measurement of trace metals in aqueous solution. *Anal. Chem.* **1995**, *67*, 3391–3400.
- (22) Santner, J.; Prohaska, T.; Luo, J.; Zhang, H. Ferrihydrite containing gel for chemical imaging of labile phosphate species in sediments and soils using diffusive gradients in thin films. *Anal. Chem.* **2010**, *82*, 7668–7674.
- (23) Boudreau, B. P. The diffusive tortuosity of fine-grained un lithified sediments. *Geochim. Cosmochim. Acta* **1996**, *60*, 3139–3142.
- (24) Harper, M. P.; Davison, W.; Zhang, H.; Tych, W. Kinetics of metal exchange between solids and solutions in sediments and soils interpreted from DGT measured fluxes. *Geochim. Cosmochim. Acta* **1998**, *62*, 2757–2770.
- (25) Murphy, J.; Riley, J. A modified single solution method for the determination of phosphate in natural waters. *Anal. Chim. Acta* **1962**, *27*, 31–36.
- (26) Santner, J.; Kreuzeder, A.; Schnepf, A.; Wenzel, W. W. Numerical Evaluation of Lateral Diffusion Inside Diffusive Gradients in Thin Films Samplers. *Environ. Sci. Technol.* **2015**, *49*, 6109–6116.
- (27) Honeyman, B. D.; Santschi, P. H. Metals in aquatic systems. *Environ. Sci. Technol.* **1988**, *22*, 862–871.
- (28) Ernstberger, H.; Davison, W.; Zhang, H.; Tye, A.; Young, S. Measurement and dynamic modeling of trace metal mobilization in soils using DGT and DIFS. *Environ. Sci. Technol.* **2002**, *36*, 349–354.
- (29) Zhang, H.; Lombi, E.; Smolders, E.; McGrath, S. Kinetics of Zn release in soils and prediction of Zn concentration in plants using diffusive gradients in thin films. *Environ. Sci. Technol.* **2004**, *38*, 3608–3613.
- (30) Zhang, H.; Davison, W.; Knight, B.; McGrath, S. In situ measurements of solution concentrations and fluxes of trace metals in soils using DGT. *Environ. Sci. Technol.* **1998**, *32*, 704–710.
- (31) Ggplot2: *Elegant Graphics for Data Analysis*; New York, 2009.
- (32) Mason, S.; McNeill, A.; McLaughlin, M. J.; Zhang, H. Prediction of wheat response to an application of phosphorus under field conditions using diffusive gradients in thin-films (DGT) and extraction methods. *Plant Soil* **2010**, *337*, 243–258.
- (33) Menezes-Blackburn, D.; et al. Organic Acids Regulation of Chemical-Microbial Phosphorus Transformations in Soils. *Environ. Sci. Technol.* **2016**, *50*, 11521–11531.
- (34) Koopmans, G.; Chardon, W.; De Willigen, P.; Van Riemsdijk, W. Phosphorus desorption dynamics in soil and the link to a dynamic concept of bioavailability. *J. Environ. Qual.* **2004**, *33*, 1393–1402.
- (35) Barros, N. F.; Comerford, N. B. Phosphorus sorption, desorption and resorption by soils of the Brazilian Cerrado supporting eucalypt. *Biomass Bioenergy* **2005**, *28*, 229–236.
- (36) Guppy, C.; Menzies, N.; Moody, P.; Blamey, F. Competitive sorption reactions between phosphorus and organic matter in soil: a review. *Soil Res.* **2005**, *43*, 189–202.
- (37) Lehto, N. J. *Diffusive Gradients in Thin-Films for Environmental Measurements*; Davison, B., Ed.; Cambridge University Press, 2016; Vol. 1, pp 146–173.
- (38) Ciffroy, P.; Nia, Y.; Garnier, J. Probabilistic multicompartmen-tal model for interpreting DGT kinetics in sediments. *Environ. Sci. Technol.* **2011**, *45*, 9558–9565.
- (39) Lehto, N. J.; Davison, W.; Zhang, H.; Tych, W. Theoretical comparison of how soil processes affect uptake of metals by diffusive gradients in thin films and plants. *J. Environ. Qual.* **2006**, *35*, 1903–1913.